Electronic Coupling Calculations for Bridge-Mediated Charge Transfer Using CDFT and Effective Hamiltonian approaches at DFT and FODFTB level

Natacha Gillet,[a,] Laura Berstis,[b] Xiaojing Wu,[c] Fruzsina Gajdos,[d] Alexander Heck,[a] Aurélien de la Lande,[c] Jochen Blumberger,[d] Marcus Elstner[a]

[a]: Institute of Physical Chemistry, Karlsruhe Institute of Technology, Kaiserstrasse 12, 76131 Karlsruhe, Germany.

[b]: National Bioenergy Center, National Renewable Energy Laboratory, 15013 Denver West Pkwy, Golden, CO, 80401 USA.

[c]: Laboratoire de Chimie-Physique, Université Paris Sud, CNRS, Université Paris Saclay, Campus d'Orsay. 15, avenue Jean Perrin, 91405 Cedex Orsay, France.

[d]: Department of Physics and Astronomy, University College London, Gower Street, London WCIE 6BT, United Kingdom.

To whom correspondence should be addressed: laura.berstis@nrel.gov, aurelien.de-la-lande@u-psud.fr, j.blumberger@ucl.ac.uk, marcus.elstner@kit.edu.

Abstract

In this article four methods to calculate charge transfer integrals in the context of bridge mediated electron transfer are tested. These methods are based on Density Functional Theory (DFT). We consider two perturbative Green's function effective Hamiltonian methods (first at the DFT level of theory using localized molecular orbitals, second applying a tight-binding DFT approach using fragment orbitals) and two constrained DFT implementations with either plane-wave or local basis sets. To assess the performance of the methods for through-bond or through-space dominated transfer, different sets of molecules are considered. For through-bond ET, several molecules that were originally synthesized by

Paddon-Row and co-workers for the deduction of electronic coupling values from photo-emission and electron transmission spectroscopies, are analysed. The tested methodologies prove to be successful in reproducing experimental data, the exponential distance decay constant and the super-bridge effects arising from interference among ET pathways. For through-space ET, dedicated π-stacked systems with heterocyclopentadienes molecules were created and analysed on the basis of electronic coupling dependence on donor-acceptor distance, structure of the bridge, and ET barrier height. The cheap FODFTB method gives similar results to CDFT and both reproduce the expected exponential decay of the coupling with donor-acceptor distances and the number of bridging units. These four approaches appear to give reliable results for both through-bonds and trough-space ET and present a good alternative to expensive *ab initio* methodologies for large systems involving long-range charge transfers.

Introduction

Long-range biological electron transfer (ET) reactions have been widely studied for decades due to their importance in biological processes such as respiration, photosynthesis and enzymatic reactions. Transfers between redox centres separated by a few to about 15 Å are facilitated by a bridge, *i.e.* the intervening medium composed of protein, solvent or other molecules. Several theoretical mechanisms have been proposed to describe ET such as bridge-mediated superexchange, charge hopping or the more recently proposed flickering resonance model.[1] The super-exchange model, involving tunnelling of the electron/hole between the donor (D) and the acceptor (A) along the bridge may be employed for the analysis of charge transfer through systems characterized by a large energy gap between the D/A and bridge (B) levels, and sufficiently short distances to permit tunnelling transport. No redox states of the bridge are directly involved in the transfer and the rate constant of the reaction is given by the following non-adiabatic Marcus's semi-classical theory equation:

$$k_{DA} = \frac{2\pi}{\hbar}\frac{1}{\sqrt{4\pi\lambda k_B T}}|T_{DA}|^2 exp\left(-\frac{(\lambda + \Delta G°)^2}{4\lambda k_B T}\right) \qquad \text{(Eq 1)}$$

where $\Delta G°$ is the driving force of the ET, λ the reorganization energy, and T_{DA} the electronic coupling between initial and final ET states. Important efforts have been made by computational chemists to develop methods to determine these three parameters at the molecular level. Since the beginning of the '80s many developments have focused on *ab initio* or semi-empirical methodologies to calculate the electronic coupling in bridge mediated ET reactions. Considering two (quasi)-diabatic states system, the electronic coupling represents the off-diagonal element of the electronic Hamiltonian matrix. Even in the presence of the bridge, the system could be diabatized in initial and final state in a two-state approximation. The problem is therefore to generate two reasonable diabatic states allowing electronic coupling calculations. One can use different methods such as block diagonalisation of the adiabatic electronic Hamiltonian,[2–4] generalized Mulliken-Hush method (GMH),[4–9] fragment charge difference,[10] fragment energy difference,[11] fragment orbital (FO),[12–19] projection methods,[20,21] constrained density functional theory (CDFT),[22–26] frozen density embedding[27], tunnelling current[19,28], etc. In addition, some multi-state diabatization techniques —i.e. three or more states including the donor, bridge and acceptor— have also been described in the literature.[29–32] Alternative less expensive approaches to determine electronic couplings are the indirect (semi-)empirical methods such as the pathway model,[33] and packing density model.[1,34]

The electronic coupling depends intrinsically upon the structure of the intervening medium. It is also known to exponentially decrease with D-A distance *d*, even in bridge mediated ET:

$$|T_{DA}| = Aexp\left(-\frac{\beta d}{2}\right) \qquad \text{(Eq 2)}$$

Since the 1980's a great deal of efforts has been devoted to the understanding of the relationships between molecular structure and electronic coupling strength, see for example References [35–40]. Two types of interactions mediate electron tunnelling along the intervening bridge: through-bond (TB) and through-space (TS) interactions. Bridges can consist of stacks of several molecules separated by vacuum,

covalently-linked molecular chains, or a mixture of both. Recent computational advancements enable high-level *ab initio* electronic coupling calculations on small systems with simple and/or symmetric bridges.[41,42] However, more complex, inhomogeneous bridge-mediated ET events, such as those occurring in diverse biological media, require computationally less expensive approaches in order to address the complexity of the medium and thermal fluctuations through many conformations. Less computationally demanding methods have thus been recently developed, based on density functional theory (DFT) or semi-empirical density functional tight-binding DFTB. To assess the necessary approximations associated with cheaper T_{DA} calculations, benchmarking analyses provide a base from which to investigate and compare the accuracy of the different methods and their respective sources of error. However, most of the existing articles focused on only one method for a given molecular system. Instead, in the present work we aim to integrate the testing and analysis of several different semi-classical methods, on a consistent set of organic D-B-A systems and compare their applicability and predictivity of T_{DA} in the various presented molecular contexts.

We have previously used several schemes, based on CDFT implemented in deMon2k or CPMD, fragment orbital density functional theory (FODFT) and density functional tight-binding (FODFTB), or an effective Hamiltonian methodology in the framework of materials science or biological systems. Recently, we published electronic coupling calculations on benchmarked D-A systems, involving hole or electron transfer,[43,44] and a study of bridge-mediated transfer through hydrocarbon molecules applying an effective Hamiltonian strategy with DFT-based Green's function pathway.[45] Electronic coupling contributions to ET through diverse biomolecules, including DNA strands,[46–49] polypeptide[50–53], heme-to-heme ET[54] or cryptochrome/photolyases,[55,56] and to organic semi-conductors[57] have been successfully calculated with these approaches. In addition to our recent works, Ando and co-workers demonstrate the utility of the fragment molecular orbital-linear combination of MOs (FMO-LCMO) for T_{DA} predictions within various organic and biological molecules.[42,58]

In this article we first review our different approaches to determine electronic couplings in D-B-A systems. We then present applications on two types of systems: (1) diene D-A systems with various covalently-bound saturated hydrocarbon bridges from Paddon-Row *et al*[59–61] to characterize coupling dominated by TB interactions, and (2) D-B-A systems involving TS interactions between unsaturated or aromatic molecules. For each D-B-A set, D and A are identical (*i.e.* the same molecule or moiety), whereas the bridge is varied by the chemical nature of its components, or by its length via the number of bridging units (whether the number of molecules or intervening covalent bonds). We compare the resulting T_{DA} predictions at different levels: within a method (for instance by the choice of a functional or a basis set), between methods or with respect to estimations from experimental data where available.

Methods

Effective Hamiltonian Methodology

In an orthogonal basis we can write the Schrödinger equation for the full D-B-A system as

$$\mathbf{HC} = E\mathbf{C} \qquad \text{(Eq 3)}$$

We then apply a partitioning scheme[62–68] where we divide the matrix equation into the D/A (a) and bridge (b) subspace:

$$\begin{pmatrix} \mathbf{H}_{aa} - E\mathbf{1}_{aa} & \mathbf{H}_{ab} \\ \mathbf{H}_{ba} & \mathbf{H}_{bb} - E\mathbf{1}_{bb} \end{pmatrix} \begin{pmatrix} \mathbf{C}_a \\ \mathbf{C}_b \end{pmatrix} = 0 \qquad \text{(Eq 4)}$$

where $\mathbf{H}_{aa}$ ($\mathbf{H}_{bb}$) is the submatrix consisting only of D/A (B) components.

There are different approaches to construct the D, A and B localized states. As implemented in GAMESS,[69] the Pipek-Mezey localization[70] routine is used in this work for orbital localizations in DFT calculations. The optimal accuracy of this localization scheme within this approach was demonstrated in previous works.[71] In FODFTB calculations, we apply fragment orbitals as localized states, which are straightforward to use when D, A and B are separated molecules.[51]

By solving one linear equation for $\mathbf{C}_b$ and substituting the result in the second equation we can reduce Eq 4 to an equivalent equation of the D/A subspace

$$\mathbf{H}_{DA}^{eff}\mathbf{C}_a = E\mathbf{C}_a \qquad \text{(Eq 5)}$$

where $\mathbf{H}_{DA}^{eff}$ is an effective (contracted) 2x2 Hamiltonian

$$\mathbf{H}_{DA}^{eff} = \mathbf{H}_{aa} + \mathbf{H}_{ab}(E\mathbf{1}_{bb} - \mathbf{H}_{bb})^{-1}\mathbf{H}_{ba} \qquad \text{(Eq 6)}$$

The Hamiltonian entering Eq 5 is therefore dependent on E, which makes a self-consistent solution necessary. The tunnelling energy E=ε_{tun} is initially set to an average of the D and A state energies, and then iteratively converged as the average of the resulting eigenvalues of the 2x2 Hamiltonian, until reaching self-consistency within a defined tolerance.

From the converged Hamiltonian, T_{DA} can be obtained as the off-diagonal element, which can be written as

$$T_{DA}(E) = \beta_{DA} + \sum_{i,j}^{B} \beta_{Di} G_{ij}(\varepsilon_{tun}) \beta_{jA} \qquad \text{(Eq 7)}$$

where β_{DA} is the direct electronic interaction between D and A, the terms β_{Di} and β_{jA} represent the interactions between the bridge and the D, and A, respectively, and G_{ij} is an element of the Green's function matrix for the bridge

$$\mathbf{G} = (\varepsilon_{tun}\mathbf{1}_{bb} - \mathbf{H}_{bb})^{-1} \qquad \text{(Eq 8)}$$

The converged eigenvalues represent the energies of the poles of the non-adiabatic intersection, at which point, the elements G_{ij}, represent the probabilities of the electron to tunnel through the specified orbital space of the bridge.[33,72–74]

Fragment-Orbital Density Functional Theory Tight-Binding

DFTB is derived from DFT using a Taylor series expansion of the total energy around a reference density, which is written as a superposition of neutral atomic densities. DFTB1,[75,76] DFTB2[77] and DFTB3[78] denote

a first, second and third-order expansion, respectively. DFTB is highly efficient both due to the application of a minimal basis and a two-centre approximation, which allows the tabulation of Hamiltonian and overlap matrix elements. In the conventional parameterization, however, the atomic basis functions are confined to achieve an optimal description of bonded situations, which in turn leads to underestimation of the electronic interactions of atoms in Van der Waals distance and beyond.[48]

In order to compensate this drawback we use a special FO description in our FODFTB calculations, which showed in previous studies inter-molecular couplings in excellent agreement with FODFT calculations in a triple-ζ basis.[43,44] As in conventional FO calculations we can obtain the FO Hamiltonian through the transformation of the Hamiltonian matrix $\mathbf{H}_{AO}$ constructed in an atomic orbital basis

$$\mathbf{H}_{FO} = \mathbf{C}^{T}\mathbf{H}_{AO}\mathbf{C} \qquad \text{(Eq 9)}$$

where **C** is a block-diagonal matrix of the fragment orbital coefficients. However, as $\mathbf{H}_{AO}$ we use in FODFTB calculations a block matrix, where the (standard) mio-1-1 parameters[77] are employed for calculation of the matrix elements in the diagonal blocks (intra-molecular interactions), and for the off-diagonal blocks (inter-molecular interactions) the same less-confined set is used as in Ref. [43] and [44]. The FO overlap matrix is obtained analogously and subsequently the submatrix of H_{FO} consisting of HOMO orbitals of the fragments is orthogonalized.

T_{DA} from Orbital Splitting

T_{DA} can also be predicted from adiabatic states. It corresponds to half of the energy gap between the ground and first excited state at the transition state geometry. In symmetrical systems, we can approximate the transition state with the optimized geometry of the neutral molecules, because the two sites are equivalent. For a non-symmetrical D-A pair, this approximation fails.[79] In a single-electron picture, one can apply Koopmans' theorem to estimate T_{DA} as half the splitting of the HOMO levels of the neutral system[72]:

$$T_{DA} = \frac{1}{2}(\varepsilon_{HOMO} - \varepsilon_{HOMO-1}) \quad \text{(Eq 10)}$$

where ε_{HOMO-1} and ε_{HOMO} correspond respectively to the energy of the ground state and of the excited state of the positively charged system.

Constrained Density Functional Theory

Constrained DFT allows one to define diabatic states at the DFT level in an *ad hoc* way.[80,81] In CDFT the energy functional minimization is performed under one or several constraints that the electron density must fulfil at SCF convergence.[82] The constraint is incorporated in the minimization process via a Lagrange multiplier technique. In Eq 10, valid for a single constraint case, $E[\rho]$ is the conventional DFT energy functional including core, Coulomb and exchange-correlation contributions (XC). λ_c is a Lagrange multiplier that needs to be determined in the SCF. Wu and Van Voorhis showed that λ_c can be obtained by maximizing the energy functional.[83] w is a real space function that determines which atoms are subjected to charge constraint and N_c is the targeted charge. Both of these terms are defined by the user. Regarding w, since there is no strict definition of an atomic charge in a molecule, one is compelled to rely on a population scheme such as those of Mulliken,[84] Löwdin[85] or Hirshfeld[86] to specify the charge constraint in practice. Past experience in our groups led us to choose the Hirshfeld scheme for the present study.

$$\mathcal{E}[\rho, \lambda_c] = \min_{\rho} \max_{\lambda_c} \left(E[\rho] + \lambda_c \left[\int \rho(\boldsymbol{r}) w(\boldsymbol{r}) d\boldsymbol{r} - N_c \right] \right) \quad \text{(Eq 11)}$$

Two implementations of constrained DFT using plane waves or localized Gaussian type atomic orbitals are tested. These two methods are implemented in CPMD[26,87] and deMon2k,[88] respectively.

Computational details

Molecular Geometries

The geometries for all ethylene, heterocyclopentadiene D-B-A structures and hydrocarbon-linked dienes were optimised in their highest symmetry conformation, C_{2V} or C_2, within the GAMESS computational chemistry software. The DFT functional B97-D[89] was employed for structural optimizations, using a very fine grid, tight convergence, and the triple-ζ basis KTZVPP.[90] Hessian vibrational analyses confirmed the positive definite structures, used in subsequent analysis across all methodologies. Cartesian coordinates of all molecules are given in Supporting Information.

DFT Effective Hamiltonian Calculations in GAMESS

The software GAMESS was used for all DFT calculations, using a very fine grid of 96 radial and 1202 angular Lebedev points. The B97-D functional[89] together with the 6-311G(2df,2pd) basis set[91] were applied for all T_{DA} calculations, given the agreeable accuracy of this level of theory found in previous work. Coupled to the Pipek-Mezey localization routine as implemented in GAMESS-US, an in-house implementation of the effective Hamiltonian calculation was utilized for electronic coupling predictions, in which the ε_{tun} convergence tolerance was set to 10^{-6} Ha.

DFTB Calculations

The FODFTB effective Hamiltonian calculations were performed with an in-house implementation of DFTB. The fragments were calculated *in vacuo* at the DFTB2 level of theory with an SCF energy convergence criterion of 10-7 Ha. The same criterion was also used for the convergence of ε_{tun}. As described in the method section, the mio-1-1 parameters were used in combination with a less confined electronic parameter set, where the density and wave function confinement radius was set to infinity and 8 bohr, respectively.[48]

Orbital splittings were obtained from standard calculations (only confined basis set) on the neutral molecule with the DFTB+ program[92] using the mio-1-1 parameters.[77] Calculations were performed at the

DFTB2 level of theory in accordance with our FODFTB implementation. The atomic charges were converged with a tolerance of 10^{-5} e between two cycles.

CDFT Calculations with deMon2k

deMon2k is based on the resolution of the Kohn-Sham equations using density fitting techniques.[93,94] When using LDA (Local Density Approximation), GGA (Generalized Gradient Approximation) functionals or hybrid GGA, the auxiliary density is further employed to calculate the XC potential and energies.[95] A variational fitting procedure of the Fock exchange potential has been used for hybrid functionals as described in Ref. [96].

For electronic coupling calculations we have tested the GGA functional PBE,[97] the meta-GGA functional TPSS[98,99] and the following hybrid GGA or meta-GGA functional PBE0[100] (25%), PBE50 (50%), B3LYP (20%),[101] BHHLYP (50%) M06-2X (54%),[102] M06HF (100%)[103] with different exchange energy replaced by Hartree-Fock exchange (HFX) as indicated in the brackets. Several Dunning "correlation-consistent" basis sets were used: the cc-pVDZ,[104] cc-pVTZ,[105] and cc-pVQZ[106] basis sets, which include polarization functions by definition, and two further augmented with diffuse functions, aug-cc-pVDZ and aug-cc-pVTZ. We also tested the influence of the basis set used to expand the auxiliary electron density including GEN-A2, GEN-A2*, GEN-A3, GEN-A3*.[107] We found little influence of the auxiliary basis set on electronic coupling values and we will only present here data obtained with GEN-A2*. SCF energy convergence criterion of 10^{-8} Ha were requested for all calculations. Convergence criterions of 10-4 e were requested for the CDFT constraints. An adaptive grid[108] was used to calculate the XC potential with a tolerance of 10-6 Ha on its diagonal matrix elements. A fixed grid of fine accuracy is specified for calculating the elements of the matrix representing the operator w (Eq. 10) with the Hirshfeld scheme.

When modelling an electron transfer reaction in a D-B-A system, two CDFT calculations must be carried out. Following Ref. [109] we found it convenient to constrain the net charge difference between D and A to equal ±1.0. Therefore in our calculation, the function w is identical for both diabatic states but the target

charge N_c is varied. There is some arbitrariness in the definition of the donor and acceptor groups in a bridge mediated ET, particularly for through bond interactions. We have consequently tested the possibility to include part of the bridge atoms in the constrained regions. Three definitions were tested for the saturated hydrocarbon bridges containing 4, 11 or 22 atoms in each donor or acceptor groups (Figure S1).

CDFT Calculations with CPMD

The CDFT calculations were also performed using the CPMD program package with a plane wave basis set. The Lagrange multiplier λ_c was optimised with the constraint set to a Hirshfeld charge difference of 1 between the donor and the acceptor group with a tolerance of $5x10^{-5}$ e. Similarly to the deMon2k calculations, the applied exchange correlation functional was PBE, where the GGA exchange was replaced with 0%, 25% and 50% exact exchange (HFX). A reciprocal space plane wave cutoff of 80 Ry was used for the orbitals and half of the cutoff for the calculation of the exact exchange energy contribution. The DBA molecules were centred in a rectangular box. The box dimensions were chosen large enough so that the distance between any nucleus and the closest box edge was at least 4.0 Å. Any further increases in box size resulted in a change of less than 0.2 meV. All calculations were done *in vacuo* by removing all interactions with periodic images. Core electrons were replaced with Troullier-Martins pseudopotentials.[110] The convergence criterion for the wavefunction optimisation was a maximum electronic gradient component of less than 10^{-7} a.u.

Results and Discussion

I. Through-bond hole transfer

Experimental and theoretical studies were performed by Paddon-Row and co-authors on a large set of nonconjugated hydrocarbon dienes, as those presented in Figure 1, to explore the orbital interactions

through several σ-bonds.[59–61] This comprehensive work emphasized the importance of TB interactions relative to TS interactions for electron transfer or hole transfer in such systems. The authors also showed the exponential decrease of electronic coupling as one increases the number of σ C-C bonds between the two diene moieties, and provided explanations for the behaviour of different bridge structures with orbital representations. Given the precedence of this experimental and theoretical data for these particular D-B-A systems, we selected the set as enumerated in Figure 1, for comparing our T_{DA} calculation approaches.

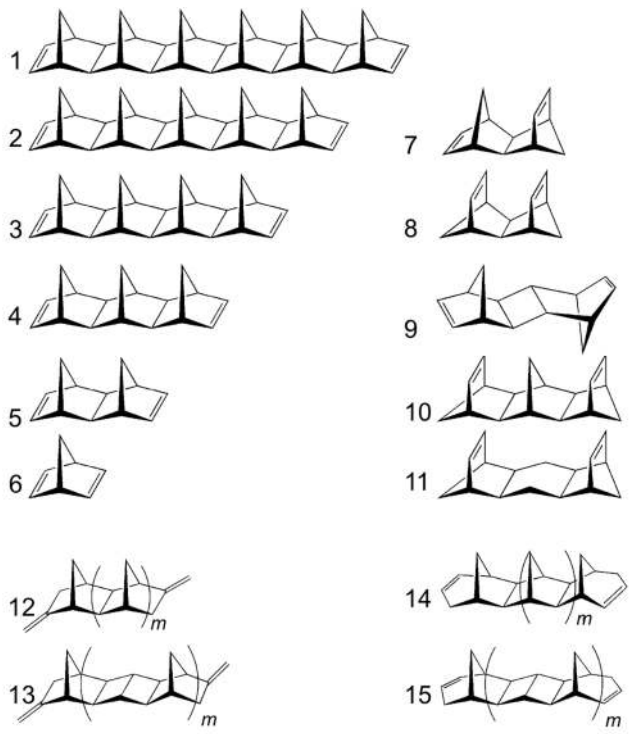

Figure 1: Molecules considered for investigating through-bond interactions.[59,61] Set 1: molecules 1-5 for variable bridge lengths; set 2: molecules 4-11, for variable bridge structures; set 3: molecules 12-15 for comparison between normal and super-bridges. *m* varies between 4 and 7 or 2 and 3 for molecules 12 and 14 or 13 and 15 respectively (corresponding to D-A distance of 11 to 17 σ-C-C bridging bonds).

We split our molecule sample into three sets. The first set comprises molecules **1** to **5** to evaluate the T_{DA} decrease with D-A distance.[60] The second set combines molecule from **4** to **11**, enables investigation of T_{DA} behaviour with variation of bridge construction. Corresponding experimental electronic couplings for this set are available from photo-emission spectroscopy (PES).[59] The third set covers molecules **12**(m) to

15(m) (between 11 and 17 σ-C-C bridging bonds) to compare T_{DA} results for polynorbornane bridges and hybrid bicyclo[2.2.0]hexane group/norbornane bridges. According to previous Hartree-Fock electronic coupling calculations, the latter bridges accelerate charge transfers by increasing the coupling and decreasing the exponential β constant.[61]

Paddon-Row and co-workers carried out photo-emission spectroscopy (PES) and electron transmission spectroscopy (ETS) experiments to respectively find the ionization potentials (IP) and electron affinities (EA) for most molecules.[59] The electronic coupling for the hole transfer case corresponds approximately to half of the π orbital splitting energy in the cationic state, as given by the IP measurement. Their studies led them to make several deductions regarding the relationship between molecular structure, and the interplay of TB *vs*. TS interactions in mediating the charge transfer. For an all-trans arrangement (molecules **4**, **5**, **9**) the maximal contribution to the ΔIP measurements comes from TB interactions. Electronic coupling for molecule **4** and **5** follows an exponential decay of 0.92 $Å^{-1}$. This TB contribution is smaller in cis-trans structures (like in molecule **7**) and minimal for all-cis bridges. However, the ΔIP is larger in molecule **8** than in molecule **7** or **5**, certainly due to a strong TS contribution between the diene stack. Even though the number of bridging bonds in molecule **6** is smaller than in molecule **5**, their experimental electronic couplings are equivalent. Indeed, the TS interactions in the norbornadiene **6** are quite strong and their contributions could oppose the TB interactions effect. The larger electronic coupling observed for molecule **10** compared to molecule **11** is attributed to laticyclic hyperconjugation, *i.e.* hyperconjugative interactions between the diene π-MO and the orbitals of the central methylene group in molecule **10**. We report these values with our electronic coupling calculations for *set 1* and *set 2* in Table 1. No experimental measurement has been found for molecule **1** to **3** and **12** to **15**.

Molecule	**Bridging Bonds**	**Exp(ref)**	**Heff**	**DFTB2**	**CDFT (deMon2k)**	**CDFT (CPMD)**

1	12	-	0.0213	0.0123	0.0177	0.023
2	10	-	0.0389	0.0215	0.0362	0.0408
3	8	-	0.0682	0.0399	0.0734	0.1128
4	6	0.16	0.1531	0.0996	0.1795	0.1913
5	4	0.44	0.4799	0.2623	0.6378	0.6230
	β(1-5)	0.92[a]	0.76 (0.99)	0.76 (0.99)	0.88 (0.99)	0.82 (0.99)
6	2	0.43	0.46	0.0884	1.0458	1.0731
7	4	0.22	0.1799	-	0.2621	0.1906
8	4	0.63	0.7509	0.3647	1.2754	1.0934
9	6	0.22	0.2459	0.1119	0.3245	0.3053
10	6	0.26	0.3322	0.1740	0.3573	0.3808
11	6	0.09	0.0964	0.0614	0.0870	0.0929
MUE (eV)			0.0319	0.0922	0.0774	0.0755
MRSE (%)			5.5	-38.4	26.3	22.7
MRUE (%)			9.8	27.4	20.6	20.4

Table 1: T_{DA} values (eV) for nonconjugated hydrocarbon dienes of set 1 (molecules 1-5) and 2 (molecules 4-11) from PES experiments[59] and calculations with DFT effective Hamiltonian (B97D/6-311g(2df, 2dp)) approach, orbital splitting at DFTB2 level and CDFT approach using deMon2k (PBE50/cc-PVTZ/GEN-A2*) or CPMD (PBE50/80 Ry) implementations. Exponential decay β (bond^{-1}) is obtained by fitting calculated electronic coupling for molecules 1 to 5; correlation coefficients are given in parenthesis. (a) Exponential decay constant obtained experimentally for all-trans arrangement molecules for a number of σ C-C bridging bonds from 3 to 6. Statistical evaluations of calculated T_{DA} couplings compared to the experimental data (except molecules 6 and 8) are given by mean of Mean Unsigned error ($MUE = \frac{1}{n}\sum_n \left|T_{DA\,calc} - T_{DA\,exp}\right|$), mean relative signed error ($MRSE = \frac{1}{n}\sum_n \frac{T_{DA\,calc} - T_{DA\,exp}}{T_{DA\,exp}}$) and mean relative unsigned error ($MRUE = \frac{1}{n}\sum_n \frac{\left|T_{DA\,calc} - T_{DA\,exp}\right|}{T_{DA\,exp}}$).

A. Test Set 1: β-decay analysis

A well-established characteristic of D-B-A electronic coupling is the mono-exponential decay with respect to the distance between D and A. The ability of our approaches to reproduce this behaviour presents an

important test of electronic coupling predictivity in D-B-A systems. *Set 1*, consisting of molecules **1** to **5**, provides a consistent series of D-B-A systems in which TB interactions predominate. The ethylene D/A moieties in **1**-**5** are separated by a decreasing number of C-C σ-bonds. The shortest molecule **6** is excluded from the series because the experimental electronic coupling value does not follow the expected exponential decay behaviour.

Optimal parameters for the DFT effective Hamiltonian approach have been previously published and discussed.[25] Meta and hybrid (with 25% HFX) functionals were found to perform well, and notable improvements were seen with the inclusion of dispersion corrections. The method was found highly sensitive to the localization ansatz, necessitating the Pipek-Mezey localization routine for accurate predictions, whereas sensitivity to basis set was determined to be relatively low. We present here tests of the different parameters (functionals, basis sets and constraint definitions) for the CDFT approach. The presence of covalent bonding between D/A and B poses a challenge for the fragmentation necessary within the FODFTB approach, nevertheless, in systems where D and A are equivalent, T_{DA} can be obtained from the HOMO splitting of standard DFTB2 calculations.

For D-A distances ranging from 3 to 6 σ bonds, experimental measurements of the electronic coupling *vs.* number of σ bonds present a β value of 0.92. Our results, presented in Figure 2, also follow an approximate exponential behaviour *vs.* D-A distances in σ bonds for which the β decays are given in Table 1. The decay values are in quite good agreement with experimental data: 0.76, 0.76, 0.82 and 0.88, for DFTB2 orbital splitting, DFT effective Hamiltonian approach, CDFT with CPMD, and CDFT with deMon2k, respectively. Correlation coefficients of around 0.99 for each approach indicate a strong correspondence of the T_{DA} values to the calculated mono-exponential curves. Orbital splitting obtained at DFTB2 level gives a qualitatively correct mono-exponential behaviour, yet with underestimated T_{DA} values. The two implementations of CDFT provide similar results. These CDFT results were obtained using hybrid PBE functional with a percentage of HFX of 50%.

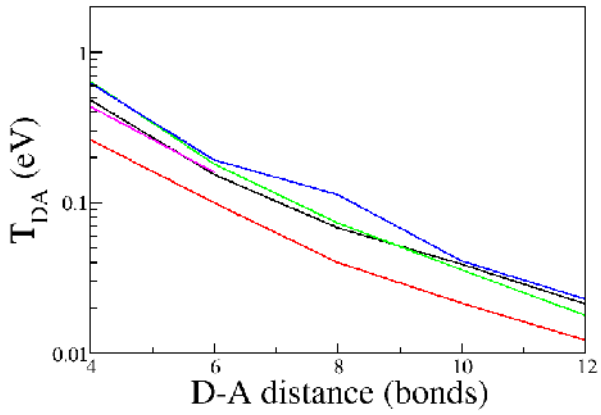

Figure 2: T_{DA} experimental values (magenta) and calculations for *set 1* with different methods: black: DFT effective Hamiltonian (B97D/6-311g(2df, 2dp)); red: orbital splitting DFTB2; green: CDFT in deMon2k (PBE50/cc-PVTZ/GEN-A2*); blue: CDFT in CPMD (PBE50/80 Ry).

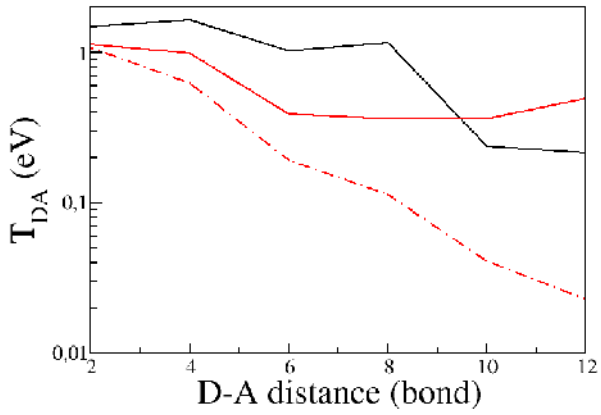

Figure 3: CDFT T_{DA} calculation for *set 1* with CPMD program and different functionals: PBE (80 Ry) black solid line; PBE0 (80 Ry) red solid line; PBE50 (80 Ry) red dotted and dashed line.

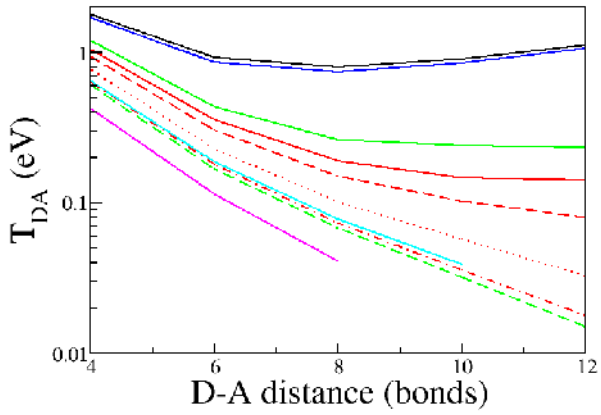

Figure 4: CDFT T_{DA} calculation for *set 1* with deMon2k program and different functionals: PBE black solid line; PBE0 red solid line; PBE30 red dashed line; PBE40 red dotted line; PBE50 red dotted and dashed line; B3LYP green solid line; BHHLYP green dashed line; TPSS blue solid line; M062X cyan solid line; M06HF magenta solid line. Calculations used cc-PVTZ basis set and GENA2* auxiliary basis set.

The importance of the amount of HFX within the CDFT approaches is further evaluated by comparing the decay curves as the percentage of HFX is adjusted. The electronic coupling correlations calculated with different functionals using the CDFT implementation in CPMD, or in the deMon2k program are represented in Figure 3 and Figure 4, respectively. Three functionals have been tested for CDFT in CPMD: PBE, PBE0 and PBE with 50% HFX. The best results are obtained with a HFX of 50%. Below this percentage, the electronic coupling is overestimated and the exponential decay is poorly reproduced. In fact, calculations with PBE yields constant T_{DA} values across the distances of 6 to 8 C-C bonds, followed by a large decrease between 8 and 10 bonds, and very small decay between 10 and 12 C-C bonds. Adding 25% HF in the exchange formulation leads to constant T_{DA} values for increasing distances from 6 to 10 C-C bonds, and then an increase of the electronic coupling at a distance of 12 C-C bonds. The importance of the percentage HFX for charge transfer has also been highlighted in a previous study.[43] Using the CDFT implementation in deMon2k, several meta-GGA and hybrid functionals were also tested. As observed in Figure 4, the quality of the β decay with D-A distance with this approach also strongly depends on the percentage of HFX. Indeed, calculations with both the PBE and TPSS functionals (which

contain no HFX) give high coupling values roughly constant for D-A distance of 6 to 12 C-C bonds. As one increases the percentage of HFX from 20% for B3LYP to 100% for M06HF, the electronic coupling value correspondingly decreases at each distance. At the same time electronic coupling dependence on D-A distance becomes closer to an exponential form. For a percentage of HFX below 40%, the electronic couplings remain high at large D-A distances, such that the curve reaches a horizontal limit. The PBE functional including 50% HFX gives similar results to experimental data, with a β value of 0.88 *vs* 0.92 experimentally. CDFT calculations using functionals with a similar amount of HFX such as M062X (54% HF) and BHHLYP (50% HF) also provide consistent electronic coupling values and decreases. Higher percentages of HFX, like for the M06HF functional, lead to stronger decay (1.18) and underestimated electronic coupling values. This dependence of the electronic coupling to the percentage of HFX can be correlated to the electronic delocalization on the molecule calculated at CDFT level. When the HFX is null or low, the electronic delocalization over the bridge is quite strong, allowing orbital overlap between the two electronic states (Figure 5). Increasing HFX fraction leads to a depopulated bridge and a less diffuse excess charge. Consequently, D/A and bridge states are less mixed and less favourable to electron tunnelling.

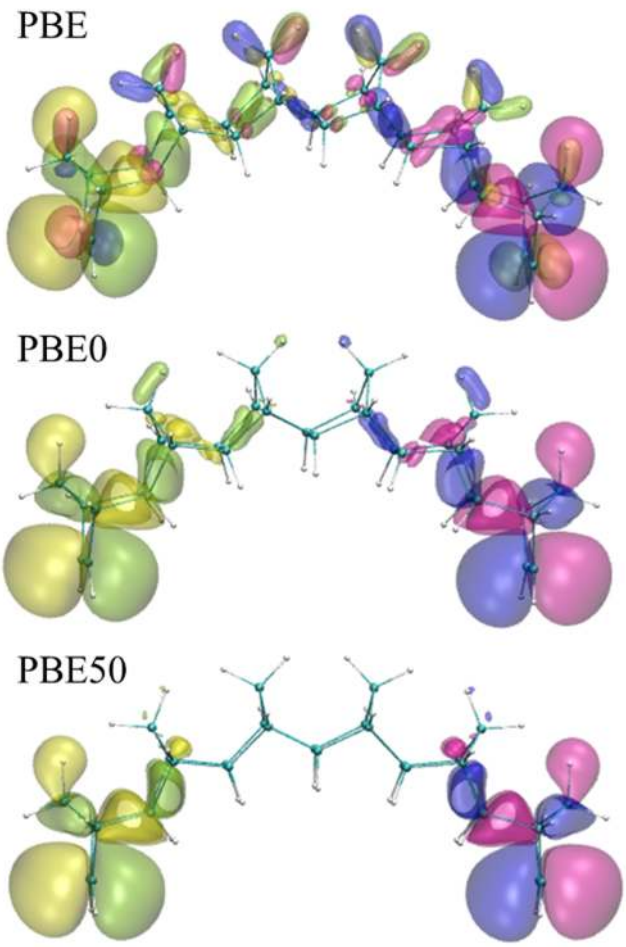

Figure 5: Single occupied Molecular Orbitals (SOMO) calculated for molecule 1 with CDFT approach in deMon2k with PBE, PBE0 and PBE50 functionals (0%, 25% and 50% HFX respectively). SOMO are obtained by a biorthogonalization procedure of the two sets of Kohn-Sham MOs.[111]

One notices that other parameters or characteristics of the functionals within the CDFT approach have nearly no influence on the electronic coupling evaluation. To fully explore these sensitivities, the electronic couplings were also calculated for different basis set (Table S4 in SI) with the deMon2k implementation. Results are highly consistent in every case, which indicates the robustness of this approach. Moreover, the results obtained with the PBE50 functional are rather insensitive to the choice of the charge constraint (see Table S5 in SI).

B. Test Set 2: Bridge conformation dependence

Experimental values deduce from ionization potential measurements are available for all the molecules of this set. All electronic coupling predictions were evaluated relative to the experimental data by calculation of mean unsigned error (MUE), mean relative signed error (MRSE) and mean relative unsigned error (MRUE).

Applying the respective optimized parameter for each approach (see previous section and ref [71]), the DFT effective Hamiltonian approach yields the lowest MUE as calculated with respect to the experimental ΔIP measurements, for this second test set. Altogether, this approach presents a MUE of 32 meV while the MUEs for others methods are around 75 to 92 meV. It is also associated to the smallest MRSE (5.5%) and MRUE (9.8%) while other methods have comparable MRUE around 20-30%. The MRUE of 9.8% within the DFT effective Hamiltonian approach was only found with the Pipek-Mezey localization, whereas all other localization routines resulted in severe overestimation of T_{DA} yielding MRUEs of approximately 50%.[71] This methodology therefore was demonstrated to be highly sensitive to the localization method in order to achieve predictions comparable to experiment.

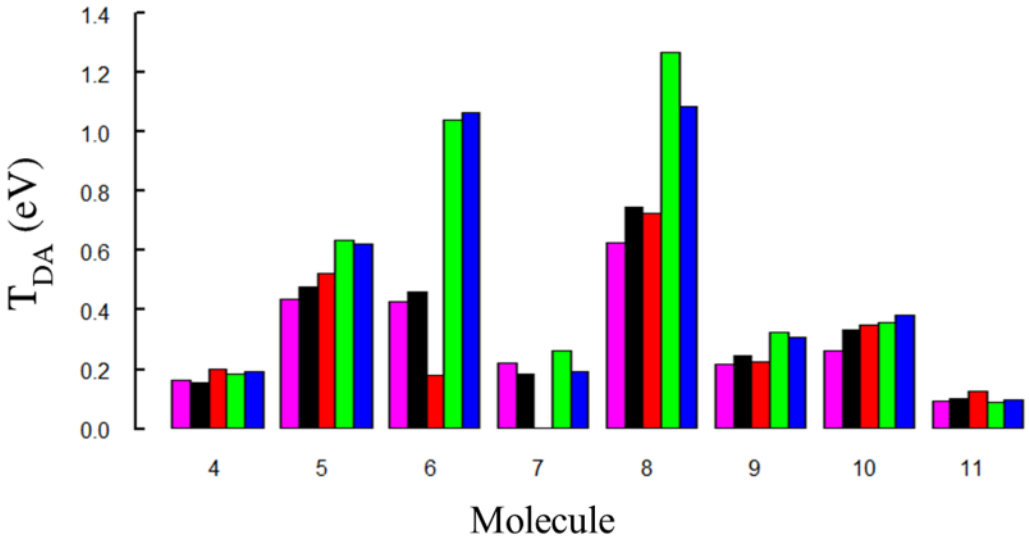

Figure 6: T_{DA} experimental values (magenta) and calculations for *set 2* with different methods: black: DFT effective Hamiltonian (B97D/6-311g(2df, 2dp)); red: orbital splitting DFTB2; green: CDFT in deMon2k (PBE50/cc-PVTZ/GEN-A2*); blue: CDFT in CPMD (PBE50/80 Ry).

For all molecules, calculations at DFBT2 level give the lowest electronic coupling and T_{DA} for molecule **7** is not calculable with an orbital splitting approach due to symmetry reasons. Nevertheless, we observe a factor close to 1.5 (corresponding to the scaling factor determined for HAB11 benchmark set with the FODFTB approach)[43,44] between DFTB2 and experimental T_{DA}, except for molecule **6** for which the factor is about 5. In contrast, all CDFT calculations give electronic coupling that are higher than experimental estimates. This difference is quite small for molecule **4**, **5**, **7**, **9**, **10** and **11** and more than twice the experimental values for the high electronic coupling of molecules **6** and **8**. In the following we would like to analyze the discrepancy between CDFT and experiment for **6** and **8** in more details.

Paddon-Row *et al* interpret that the TS interactions between the two diene groups are more important than in the other molecules, where TB interactions primarily mediate the electronic coupling. From an ET/hole perspective, molecule **8** is essentially a stacked ethylene dimer and the hole transfer occurs mainly via TS interactions. As previously reported, the CDFT (CPMD/PBE50 methodology could reproduce very well *ab*-initio electronic couplings at the MRCI level for hole transfer in stacked ethylene dimers.[43] The coupling obtained from CDFT (CPMD/PBE50) at 3.5 Å was 0.5569 eV *vs* 0.5192 eV from MRCI. Similarly the exponential decay constant was well reproduced, 2.8 $Å^{-1}$ from CDFT vs 2.7 $Å^{-1}$ from MRCI. Using this CDFT β value, the electronic coupling for an ethylene dimer in a stacked configuration with a separation of about 3.0 Å as in molecule **8** should be 1.108 eV. This compares extremely well with our CDFT electronic coupling values for molecule **8**. Likewise, TS interaction in molecule **6** will be well described. In fact, the CDFT coupling value obtained (1.05 eV) is close to the one obtained by extrapolation of the exponential distance decay relation for molecules **1-5** (1.2 eV). Besides, it is very surprising that the coupling of molecule **6** should be the same as the one for molecule **5**, as the experimental values suggest, given that the number of covalent bonds between donor and acceptor is

smaller in **6** than in **5** and the additional TS contribution in **6**. Hence, while computed values need to be considered with care due to the non-uniqueness of diabatic states, choice of constraint and sensitivity on functional, there is some strong theoretical support for the CDFT electronic coupling values obtained for **6** and **8**. Besides, experimental procedures for determination of electronic couplings could be called into question, too. The experimental data are not from direct measurements of the electronic coupling, but rather deduced from IP measurements, which come with their respective sources of error. Therefore in our error analysis reported in Table 1, molecules **6** and **8** were not included.

All of the compared methods are able to reproduce relative behaviour of the experimental electronic coupling such as the decrease between all-trans molecule and cis-trans (between molecule **5** and **7**) or the laticyclic hyperconjugative interaction effects in molecule **10** compared to molecule **11**.

C. Test Set 3: normal versus superbridge

The bridge structure has also been shown to dramatically modify electronic coupling. By inserting a bicyclo[2.2.0]hexane group between the norbornane moieties, Paddon-Row *et al* modelled superbridge molecules. This modification results in a markedly increased coupling, with concomitant decrease of the β value in comparison to the polynorbornane bridge. We selected two of these "superbridge" systems and their normal bridge equivalents, which differ with respect to their terminal diene moiety arrangements (Figure 1).

We previously showed that both implementations of CDFT give similar results for electronic coupling. Consequently, we focus on this part only on CDFT approach with deMon2k. No experimental data exists to validate our calculations on these superbridge systems; however, we can compare them to the results obtained and discussed by Paddon-Row and co-workers.[59] They theoretically determined orbital splitting energies at the HF/3-21G level of theory, and applied the Natural Bond Orbital (NBO) technique to analyse the TB coupling.

Molecule	Bridging Bonds	HF	CDFT
12	11	0.0630	0.0301
	13	0.0459	0.0181
	15	0.0332	0.0110
	17	0.0251	0.0067
	β	0.30	0.50
13	11	0.1295	0.0617
	15	0.1055	0.0277
	β	0.10	0.40
14	11	0.0557	0.0273
	13	0.0411	0.0162
	15	0.0297	0.0097
	17	0.0215	0.0059
	β	0.32	0.52
15	11	0.1200	0.0534
	15	0.0945	0.0273
	β	0.12	0.34

Table 2: T_{DA} values (eV) for nonconjugated hydrocarbon dienes of set 3 calculated at HF/3-21G (HF)[61] or CDFT/PBE50/cc-PVTZ level (CDFT).

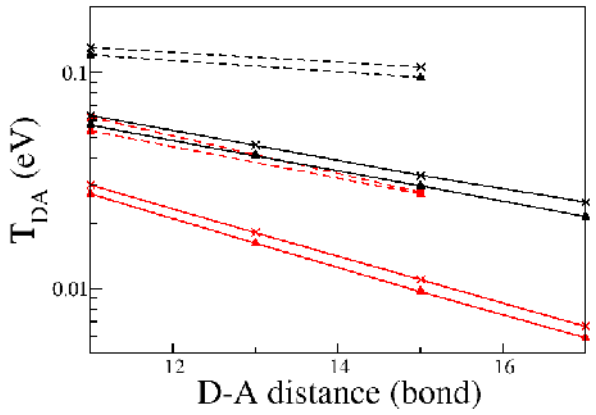

Figure 7: Electronic coupling for polynorbornane (solid line) and superbridge molecules (dashed line) from set 3 from ref [61] (black) and CDFT calculations at PBE50/cc-PVTZ/GEN-A2* level with deMon2k (red). Cross symbols refer to 12 and 13 molecules and triangles to 14 and 15.

CDFT calculations give smaller electronic coupling values and stronger β values than the NBO approach in every case. Nevertheless, the "superbridge" effect is reproduced quite well, yielding nearly doubled T_{DA} predictions for molecules **13** and **15,** compared to their standard bridge counterparts **12** and **14,** respectively. The "superbridge" effect on the β value is less important with the CDFT approach than for HF calculation, but a substantial modification of the decay constant of 0.10 and 0.18 per bond is observed for the **12**/**13** and **14/15** pairs respectively (found to be 0.20 per bond with the HF method). As the two approaches are based on different methodologies, the "superbridge" character of molecules **13** and **15** is further supported by our CDFT calculations. Our tests also underline that CDFT methods are able to reproduce the constructive inter-relay interference mentioned in ref [61]. Another interesting point is the strongly correlated mono-exponential decay observed even at large distances. As such, the electronic couplings are found predictive even at the meV scale.

II. Through space hole transfer

We now focus on hole transfer through non-covalent bridges. Straightforward models for such transfer consist of stacked small unsaturated molecules. The distance between donor and acceptor can vary as well as the number of bridging molecules. In order to achieve optimal coupling for effective T_{DA} modelling, we chose parallel stacks of bridge molecules to mediate the electronic coupling. The donor and acceptor are the same species, with bridging molecules of different character, (e.g., substitution of hydrogen atoms, or modification of heteroatoms.) The angle between the π-system has obviously a great influence on the electronic coupling, but here we focus only on the impact of the distance parameter by leaving the stacks parallel.

In order to be only a mediator, the bridge must be a worse electron donor than the D-A molecules. When this is not the case, electronic coupling calculations could fail, not converge, or lead to irrelevant values. Our models were therefore first evaluated for the consistency of their ionization potentials (IP), to construct effective D-B-A pairings. Initially, stacks of fluorinated ethylene (D-A) and ethylene (B) molecules were investigated. Substitution of two or four hydrogen atoms by fluorine atoms should very slightly decrease the vertical IP. Nevertheless, depending on the method, and in particular on the percentage of HFX in the calculation of the electronic density, different trends were observed. Experimental data show similar IP for ethylene and fluoroethylene;[112] ethylene HOMO is energetically higher than fluoroethylene one for PBE and DFTB2 while Hartree-Fock calculation give the opposite order (Table S6 in SI). Consequently, given this disagreement in IP, fluoroethylene/ethylene stacked systems were inadequate candidates for evaluating predictions at different theoretical levels.

We then considered another group of D-B-A system involving now heterocyclopentadiene such as pyrrole, imidazole or furane. To avoid a barrierless electron transfer to the bridge, we first performed calculations of the ionization potential (IP) and of the HOMO energy for each selected molecule at DFT level with various functionals. We thus also test the stability of the IP differences towards the functional used and the percentage of HFX and choose candidates for D-B-A systems. Electronic couplings for ET

transfers in heterocyclopentadiene dimers are previously evaluated in the framework of benchmarks studies on the HAB11 database.[43]

We thus created parallel π-stacked systems to measure how the electronic coupling is affected by (1) the barrier height given as IP or HOMO energy difference, (2) increasing the distance between D-B-A molecules, and (3) extending the bridge with additional bridging molecules (Figure 8). These systems are specifically designed to test our different methods for coupling calculations. The distance between each heterocyclopentadiene is of 3.5 Å (for **1**, **2**, **3**, **6**, **7**) or 3.5 + n Å (for **4** and **5**, with n=1 and 2 respectively, n=3 leading to very small electronic couplings). In the previous section, we observed that the two implementations of CDFT in CPMD or deMon2k give very similar results. The Pipek-Mezey localization of the DFT effective Hamiltonian method is not suitable for the description of delocalized D/A orbitals in these π-conjugated stacks. Therefore, we will discuss here only CDFT results from deMon2k implementation and compare it with FODFTB effective Hamiltonian calculations. At CDFT level, we will use only PBE50 functional and cc-PVTZ basis set.

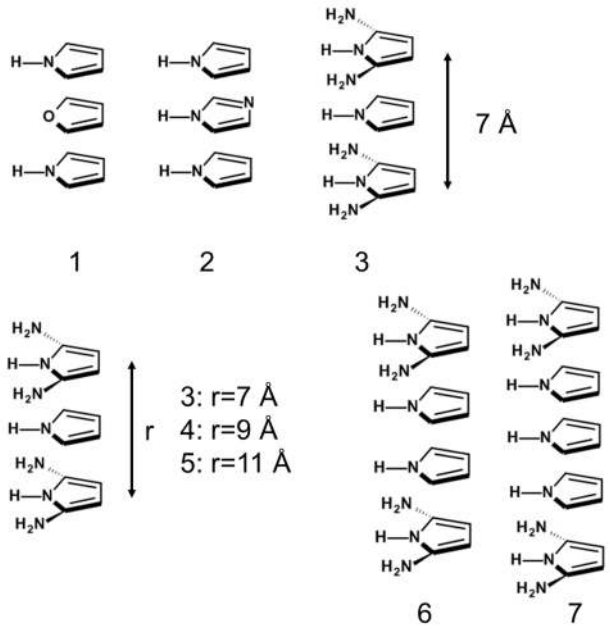

Figure 8: Heterocyclopentadiene stacks. First set (molecular systems 1, 2 and 3) for influence of the nature of D-A and B. Second set (molecular systems 3, 4 and 5) for D-A distance influence. Third set (molecular systems 3, 6, 7) for influence of the number of bridging molecules.

system		CDFT (DFT)	FODFTB (DFTB2)
1	**7 Å**	0.0961 (0.666)	0.1580 (0.416)
2	**7 Å**	0.0849 (0.678)	0.1700 (0.330)
3	**7 Å**	0.0777 (0.553)	0.0804 (0.652)
4	**9 Å**	0.0040	0.0031
5	**11 Å**	0.0001	0.00006
	β(3,4,5)	3.28	2.60
6	**10.5 Å**	0.0251	0.0412
7	**14 Å**	0.0085	0.0221
	β(3,6,7)	0.62	0.36

Table 3: T_{DA} values (eV) for cyclopentadiene stacks and the exponential decay constant β ($Å^{-1}$) calculated with the CDFT (PBE50/cc-PVTZ/GEN-A2*) and FODFTB approaches. For system 1, 2 and 3 the barrier height (Eq 11), respectively calculated at DFT(PBE50/cc-PVTZ/GEN-A2*) and DFTB2 level, is given in eV in parenthesis.

A. Test Set 1: influence of the chemical nature

The first set contains systems that differ with respect to the molecular bridge. The molecules are selected in a way that the individual stacks in this set constitute different barrier heights. We can define the barrier height as

$$\Delta E = IP_B - IP_{D/A} \qquad \text{(Eq 12)}$$

where IP_B and $IP_{D/A}$ are the vertical ionization potential of B and D-A molecules respectively. In Table 3, DFT level, we can observe that the barrier follows a **2 > 1** > **3** order while the electronic coupling slightly decreases from system **1** to system **3**. This unexpected behaviour is independent of the functional and may partly result from our definition of ΔE, which is calculated from the IP of isolated molecules *in vacuo*, whereas in the complex interactions with neighbouring molecules would affect the IP of the individual molecules. Effective Hamiltonian calculations with the FODFTB approach give more consistent results

with a decreasing T_{DA} for an increasing barrier. Nevertheless, both methodologies give similar barrier heights and T_{DA} values for system **3**. For further distance-dependence analysis, system **3** has been then modified by increasing D/A distance (molecular systems **4** and **5**) and including more bridging molecules (systems **6** and **7**).

B. Test Set 2: β decay analysis

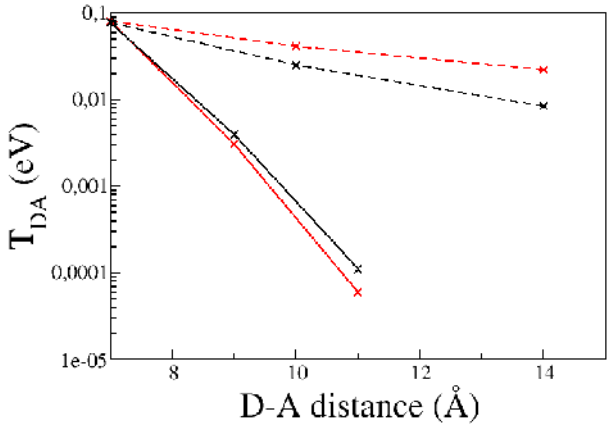

Figure 9: T_{DA} values for set 2 (solid lines) and 3 (dashed lines) calculated with CDFT (PBE50/cc-PVTZ/GEN-A2*; deMon2k implementation) (black) and FODFTB approaches (red).

The second set allows us to describe the electronic coupling dependence with the D-A distance, while keeping the same bridging molecule. Calculated electronic couplings are presented in Figure 9 (solid lines). Despite a slight difference increasing with D-A distance, which can be attributed to polarization effects at large distances, both methods give the same tendency for modulations of the electronic couplings. An exponential decay with a β value of 3.28 $Å^{-1}$ and 2.60 $Å^{-1}$ is observed for the CDFT and FODFTB approaches, respectively. As expected, these decays are stronger for these TS interactions than for the TB interactions studied in the first part of this work and similar to decays for D-A heterocyclopentadiene dimers (about 2.8-3 $Å^{-1}$).

C. Test Set 3: increasing bridge units

The last set includes systems with an increasing number of bridging molecules, the nature of these molecules, and the distance between them remaining the same. An exponential decrease of the electronic

coupling is also expected but the presence of several bridging molecule must decrease β values and ensure a better coupling at large distance. Indeed, we observe a decay value of 0.62 $Å^{-1}$ and 0.36 $Å^{-1}$ for CDFT and FODFTB respectively.

Conclusion

Characterization of TB-mediated coupling predictions with all methodologies revealed correct qualitative decay and relative trends in electronic coupling with respect to the bridge construction and D-A distance, when applying optimal conditions for each approach. As previously demonstrated, using a hybrid functional with 50% HFX gives the best results for the CDFT approach in both of our implementations. Lower HFX percentage could lead to an overestimation of the electronic delocalization, and a non-exponential decay of the electronic coupling with the distance. Basis set and definition of the constraint do not affect the accuracy of the electronic coupling significantly. Basis set insensitivity here is due to the bridge providing sufficient basis set functions between donor and acceptor. On the contrary, tunnelling through vacuum is quite basis set dependent for Gaussian basis sets, because a small Gaussian basis set does not reproduce the tails very well. While the DFT effective Hamiltonian method has been shown to have strong dependence upon the localization routine, lesser sensitivities are observed with respect to basis set. Questions regarding the accuracy of the experimental measurements were substantiated by high-accuracy calculations of bridged ethylene moieties. As such, comparisons of quantitative accuracy with respect to the experimental predictions are less relevant than the demonstrated ability of each approach to reproduce the qualitative trends in T_{DA} predictions. This points to the need for improved experimental measurements of simple hydrocarbon systems for future theoretical-experimental benchmarking purposes. The significant increases in electronic coupling for the superbridge variations of these TB-coupled ethylenes were correctly reproduced.

The set of heterocyclopentadiene D-B-A systems, designed to evaluate TS-mediated coupling, demonstrated the ability of the FODFTB effective Hamiltonian and CDFT approaches to model the correct barrier heights, and T_{DA} behaviour consistent with D-A distance and number of bridging

molecules. The two studied effective Hamiltonian methods show their strength in the TB and TS set of molecules, respectively. The FODFTB method uses HOMOs of the individual fragments, which is a natural basis for the TS transfer in non-covalent systems, but fragmentation gets problematic for covalently bound systems. The Pipek-Mezey localization of the DFT effective Hamiltonian method, on the other hand, allows the construction of bond-localized D/A orbitals in the covalent TB systems, but cannot describe the delocalized D/A orbitals of π-conjugated systems.

Associated Content

Optimized geometries of the different molecules used for T_{DA} calculation. Detailed results of functionals, basis and constraint comparisons.

Acknowledgements

CDFT calculations with the CPMD program were carried out on ARCHER, the UK National High Performance Computing facility (Edinburgh, UK), to which access was granted via the Materials Chemistry Consortium (Engineering and Physical Sciences Research Council grant No. EP/L000202). Effective Hamiltonian calculations within GAMESS performed using supercomputer time provided by the NREL Computational Sciences Center, which is supported by the DOE Office of EERE under Contract No. DE-AC36- 08GO28308. N. G. acknowledges the Alexander v. Humboldt foundation for support.

References

(1) Blumberger, J. Recent Advances in the Theory and Molecular Simulation of Biological Electron Transfer Reactions. *Chem. Rev.* **2015**, *115*, 11191–11238.
(2) Pacher, T.; Cederbaum, L. S.; Köppel, H. Approximately Diabatic States from Block Diagonalization of the Electronic Hamiltonian. *J. Chem. Phys.* **1988**, *89*, 7367–7381.
(3) Domcke, W.; Woywod, C. Direct Construction of Diabatic States in the CASSCF Approach. Application to the Conical Intersection of the 1A2 and 1B1 Excited States of Ozone. *Chem. Phys. Lett.* **1993**, *216*, 362–368.
(4) Cave, R. J.; Newton, M. D. Calculation of Electronic Coupling Matrix Elements for Ground and Excited State Electron Transfer Reactions: Comparison of the Generalized Mulliken–Hush and Block Diagonalization Methods. *J. Chem. Phys.* **1997**, *106*, 9213–-9226.
(5) Cave, R. J.; Newton, M. D. Generalization of the Mulliken-Hush Treatment for the Calculation of Electron Transfer Matrix Elements. *Chem. Phys. Lett.* **1996**, *249*, 15–19.
(6) Mulliken, R. S. Molecular Compounds and Their Spectra. II. *J. Am. Chem. Soc.* **1952**, *74*, 811–824.

(7) Hush, N. S. Homogeneous and Heterogeneous Optical and Thermal Electron Transfer. *Electrochimica Acta* **1968**, *13*, 1005–1023.
(8) Reimers, J. R.; Hush, N. S. Electronic Properties of Transition-Metal Complexes Determined from Electroabsorption (Stark) Spectroscopy. 2. Mononuclear Complexes of ruthenium(II). *J. Phys. Chem.* **1991**, *95*, 9773–9781.
(9) Creutz, C.; Newton, M. D.; Sutin, N. Metal—lingad and Metal—metal Coupling Elements. *J. Photochem. Photobiol. Chem.* **1994**, *82*, 47–59.
(10) Voityuk, A. A.; Rösch, N. Fragment Charge Difference Method for Estimating Donor–acceptor Electronic Coupling: Application to DNA π-Stacks. *J. Chem. Phys.* **2002**, *117*, 5607–5616.
(11) Hsu, C.-P.; You, Z.-Q.; Chen, H.-C. Characterization of the Short-Range Couplings in Excitation Energy Transfer. *J. Phys. Chem. C* **2008**, *112*, 1204–1212.
(12) Farazdel, A.; Dupuis, M.; Clementi, E.; Aviram, A. Electric-Field Induced Intramolecular Electron Transfer in Spiro .pi.-Electron Systems and Their Suitability as Molecular Electronic Devices. A Theoretical Study. *J. Am. Chem. Soc.* **1990**, *112*, 4206–4214.
(13) Senthilkumar, K.; Grozema, F. C.; Bickelhaupt, F. M.; Siebbeles, L. D. A. Charge Transport in Columnar Stacked Triphenylenes: Effects of Conformational Fluctuations on Charge Transfer Integrals and Site Energies. *J. Chem. Phys.* **2003**, *119*, 9809-9817.
(14) Zeng, X.; Hu, X.; Yang, W. Fragment-Based Quantum Mechanical/Molecular Mechanical Simulations of Thermodynamic and Kinetic Process of the Ru $^{2+}$ –Ru $^{3+}$ Self-Exchange Electron Transfer. *J. Chem. Theory Comput.* **2012**, *8*, 4960–4967.
(15) Smith, D. M. A.; Rosso, K. M.; Dupuis, M.; Valiev, M.; Straatsma, T. P. Electronic Coupling between Heme Electron-Transfer Centers and Its Decay with Distance Depends Strongly on Relative Orientation. *J. Phys. Chem. B* **2006**, *110*, 15582–15588.
(16) Oberhofer, H.; Blumberger, J. Insight into the Mechanism of the $Ru^{2+\$}$-$Ru^{3+\$}$ Electron Self-Exchange Reaction from Quantitative Rate Calculations. *Angew Chem Int Ed* **2010**, *49*, 3631–3634.
(17) Oberhofer, H.; Blumberger, J. Revisiting Electronic Couplings and Incoherent Hopping Models for Electron Transport in Crystalline C_{60} at Ambient Temperatures. *Phys Chem Chem Phys* **2012**, *14*, 13846–13852.
(18) Schober, C.; Reuter, K.; Oberhofer, H. Critical Analysis of Fragment-Orbital DFT Schemes for the Calculation of Electronic Coupling Values. *J Chem Phys* **2016**, *144*, 54103–54114.
(19) Gajdos, F.; Valner, S.; Hoffmann, F.; Spencer, J.; Breuer, M.; Kubas, A.; Dupuis, M.; Blumberger, J. Ultrafast Estimation of Electronic Couplings for Electron Transfer between Pi-Conjugated Organic Molecules. *J Chem Theory Comput* **2014**, *10*, 4653–4660.
(20) Migliore, A.; Corni, S.; Di Felice, R.; Molinari, E. First-Principles Density-Functional Theory Calculations of Electron-Transfer Rates in Azurin Dimers. *J. Chem. Phys.* **2006**, *124*, 64501–64516.
(21) Migliore, A.; Sit, P. H.-L.; Klein, M. L. Evaluation of Electronic Coupling in Transition-Metal Systems Using DFT: Application to the Hexa-Aquo Ferric−Ferrous Redox Couple. *J. Chem. Theory Comput.* **2009**, *5*, 307–323.
(22) Wu, Q.; Van Voorhis, T. Extracting Electron Transfer Coupling Elements from Constrained Density Functional Theory. *J. Chem. Phys.* **2006**, *125*, 164105–164113.
(23) Wu, Q.; Van Voorhis, T. Constrained Density Functional Theory and Its Application in Long-Range Electron Transfer. *J. Chem. Theory Comput.* **2006**, *2*, 765–774.
(24) de la Lande, A.; Salahub, D. R. Derivation of Interpretative Models for Long Range Electron Transfer from Constrained Density Functional Theory. *J. Mol. Struct. THEOCHEM* **2010**, *943*, 115–120.
(25) Oberhofer, H.; Blumberger, J. Charge Constrained Density Functional Molecular Dynamics for Simulation of Condensed Phase Electron Transfer Reactions. *J. Chem. Phys.* **2009**, *131*, 64101–64111.

(26) Oberhofer, H.; Blumberger, J. Electronic Coupling Matrix Elements from Charge Constrained Density Functional Theory Calculations Using a Plane Wave Basis Set. *J. Chem. Phys.* **2010**, *133*, 244105–244114.
(27) Pavanello, M.; Neugebauer, J. Modelling Charge Transfer Reactions with the Frozen Density Embedding Formalism. *J. Chem. Phys.* **2011**, *135*, 234103–234115.
(28) Stuchebrukhov, A. A. Long-Distance Electron Tunneling in Proteins. *Theor. Chem. Acc.* **2003**, *110*, 291–306.
(29) Voityuk, A. A. Estimation of Electronic Coupling in π-Stacked Donor-Bridge-Acceptor Systems: Correction of the Two-State Model. *J. Chem. Phys.* **2006**, *124*, 64505–64510.
(30) Subotnik, J. E.; Yeganeh, S.; Cave, R. J.; Ratner, M. A. Constructing Diabatic States from Adiabatic States: Extending Generalized Mulliken–Hush to Multiple Charge Centers with Boys Localization. *J. Chem. Phys.* **2008**, *129*, 244101–244111.
(31) Zusman, L. D.; Beratan, D. N. Electron Transfer in Three-Center Chemical Systems. *J. Chem. Phys.* **1999**, *110*, 10468–10481.
(32) Yang, C.-H.; Hsu, C.-P. A Multi-State Fragment Charge Difference Approach for Diabatic States in Electron Transfer: Extension and Automation. *J. Chem. Phys.* **2013**, *139*, 154104.
(33) J N Onuchic; D N Beratan; J R Winkler; Gray, H. B. Pathway Analysis of Protein Electron-Transfer Reactions. *Annu. Rev. Biophys. Biomol. Struct.* **1992**, *21*, 349–377.
(34) Hopfield, J. J. Electron Transfer Between Biological Molecules by Thermally Activated Tunneling. *Proc. Natl. Acad. Sci.* **1974**, *71*, 3640–3644.
(35) Beratan, D. N.; Onuchic, J. N.; Hopfield, J. J. Electron Tunneling through Covalent and Noncovalent Pathways in Proteins. *J. Chem. Phys.* **1987**, *86*, 4488.
(36) Beratan, D. N.; Betts, J. N.; Onuchic, J. N. Tunneling Pathway and Redox-State-Dependent Electronic Couplings at Nearly Fixed Distance in Electron Transfer Proteins. *J. Phys. Chem.* **1992**, *96*, 2852–2855.
(37) Slowinski, K.; Chamberlain, R. V.; Miller, C. J.; Majda, M. Through-Bond and Chain-to-Chain Coupling. Two Pathways in Electron Tunneling through Liquid Alkanethiol Monolayers on Mercury Electrodes. *J. Am. Chem. Soc.* **1997**, *119*, 11910–11919.
(38) Oevering, H.; Paddon-Row, M. N.; Heppener, M.; Oliver, A. M.; Cotsaris, E.; Verhoeven, J. W.; Hush, N. S. Long-Range Photoinduced through-Bond Electron Transfer and Radiative Recombination via Rigid Nonconjugated Bridges: Distance and Solvent Dependence. *J. Am. Chem. Soc.* **1987**, *109*, 3258–3269.
(39) Paddon-Row, M. N. Investigating Long-Range Electron-Transfer Processes with Rigid, Covalently Linked Donor-(Norbornylogous Bridge)-Acceptor Systems. *Acc. Chem. Res.* **1994**, *27*, 18–25.
(40) Newton, M. D. Quantum Chemical Probes of Electron-Transfer Kinetics: The Nature of Donor-Acceptor Interactions. *Chem. Rev.* **1991**, *91*, 767–792.
(41) Hsu, C.-P. The Electronic Couplings in Electron Transfer and Excitation Energy Transfer. *Acc. Chem. Res.* **2009**, *42*, 509–518.
(42) Nishioka, H.; Ando, K. Electronic Coupling Calculation and Pathway Analysis of Electron Transfer Reaction Using Ab Initio Fragment-Based Method. I. FMO–LCMO Approach. *J. Chem. Phys.* **2011**, *134*, 204109–204120.
(43) Kubas, A.; Hoffmann, F.; Heck, A.; Oberhofer, H.; Elstner, M.; Blumberger, J. Electronic Couplings for Molecular Charge Transfer: Benchmarking CDFT, FODFT, and FODFTB against High-Level Ab Initio Calculations. *J. Chem. Phys.* **2014**, *140*, 104105–104125.
(44) Kubas, A.; Gajdos, F.; Heck, A.; Oberhofer, H.; Elstner, M.; Blumberger, J. Electronic Couplings for Molecular Charge Transfer: Benchmarking CDFT, FODFT and FODFTB against High-Level Ab Initio Calculations. II. *Phys Chem Chem Phys* **2015**, *17*, 14342–14354.
(45) Berstis, L.; Baldridge, K. K. DFT-Based Green's Function Pathways Model for Prediction of Bridge-Mediated Electronic Coupling. *Phys. Chem. Chem. Phys.* **2015**, *17*, 30842–30853.

(46) Rösch, N.; Voityuk, A. A. Quantum Chemical Calculation of Donor-Acceptor Coupling for Charge Transfer in DNA. *Top Curr Chem* **2004**, *237*, 37–72.
(47) Troisi, A.; Orlandi, G. The Hole Transfer in DNA: Calculation of Electron Coupling between Close Bases. *Chem. Phys. Lett. 344*, 509–518.
(48) Kubař, T.; Woiczikowski, P. B.; Cuniberti, G.; Elstner, M. Efficient Calculation of Charge-Transfer Matrix Elements for Hole Transfer in DNA. *J. Phys. Chem. B* **2008**, *112*, 7937–7947.
(49) Kubař, T.; Elstner, M. What Governs the Charge Transfer in DNA? The Role of DNA Conformation and Environment. *J. Phys. Chem. B* **2008**, *112*, 8788–8798.
(50) Heck, A.; Woiczikowski, P. B.; Kubař, T.; Giese, B.; Elstner, M.; Steinbrecher, T. B. Charge Transfer in Model Peptides: Obtaining Marcus Parameters from Molecular Simulation. *J. Phys. Chem. B* **2012**, *116*, 2284–2293.
(51) Heck, A.; Woiczikowski, P. B.; Kubař, T.; Welke, K.; Niehaus, T.; Giese, B.; Skourtis, S.; Elstner, M.; Steinbrecher, T. B. Fragment Orbital Based Description of Charge Transfer in Peptides Including Backbone Orbitals. *J. Phys. Chem. B* **2014**, *118*, 4261–4272.
(52) Řezáč, J.; Lévy, B.; Demachy, I.; de la Lande, A. Robust and Efficient Constrained DFT Molecular Dynamics Approach for Biochemical Modeling. *J. Chem. Theory Comput.* **2012**, *8*, 418–427.
(53) Berstis, L.; Beckham, G. T.; Crowley, M. F. Electronic Coupling through Natural Amino Acids. *J. Chem. Phys.* **2015**, *143*, 225102.
(54) Breuer, M.; Rosso, K. M.; Blumberger, J. Electron Flow in Multiheme Bacterial Cytochromes Is a Balancing Act between Heme Electronic Interaction and Redox Potentials. *Proc. Natl. Acad. Sci.* **2014**, *111*, 611–616.
(55) Lüdemann, G.; Solov'yov, I. A.; Kubař, T.; Elstner, M. Solvent Driving Force Ensures Fast Formation of a Persistent and Well-Separated Radical Pair in Plant Cryptochrome. *J. Am. Chem. Soc.* **2015**, *137*, 1147–1156.
(56) Cailliez, F.; Müller, P.; Firmino, T.; Pernot, P.; de la Lande, A. Energetics of Photoinduced Charge Migration within the Tryptophan Tetrad of an Animal (6–4) Photolyase. *J. Am. Chem. Soc.* **2016**, *138*, 1904–1915.
(57) Heck, A.; Kranz, J. J.; Kubař, T.; Elstner, M. Multi-Scale Approach to Non-Adiabatic Charge Transport in High-Mobility Organic Semiconductors. *J. Chem. Theory Comput.* **2015**, *11*, 5068–5082.
(58) Kitoh-Nishioka, H.; Ando, K. Fragment Molecular Orbital Study on Electron Tunneling Mechanisms in Bacterial Photosynthetic Reaction Center. *J. Phys. Chem. B* **2012**, *116*, 12933–12945.
(59) Balaji, V.; Ng, L.; Jordan, K. D.; Paddon-Row, M. N.; Patney, H. K. Study of Long-Range .pi.*,.pi.* Interactions in Rigid Molecules by Electron Transmission Spectroscopy. *J. Am. Chem. Soc.* **1987**, *109*, 6957–6969.
(60) Jordan, K. D.; Paddon-Row, M. N. Long-Range Interactions in a Series of Rigid Nonconjugated Dienes. 1. Distance Dependence of the .pi.+,.pi.- and .pi.+*,.pi.-* Splittings Determined from Ab Initio Calculations. *J. Phys. Chem.* **1992**, *96*, 1188–1196.
(61) Paddon-Row, M. N.; Shephard, M. J. Through-Bond Orbital Coupling, the Parity Rule, and the Design of "Superbridges" Which Exhibit Greatly Enhanced Electronic Coupling: A Natural Bond Orbital Analysis. *J. Am. Chem. Soc.* **1997**, *119*, 5355–5365.
(62) Teklos, A.; Skourtis, S. S. Comparative Study of Perturbative Methods for Computing Electron Transfer Tunneling Matrix Elements with a Nonorthogonal Basis Set. *J. Chem. Phys.* **2006**, *125*, 244103–244111.
(63) Teklos, A.; Skourtis, S. S. Erratum: "Comparative Study of Perturbative Methods for Computing Electron Transfer Tunneling Matrix Elements with a Nonorthogonal Basis Set" [J. Chem. Phys. 125, 244103 (2006)]. *J. Chem. Phys.* **2007**, *126*, 209902.
(64) Löwdin, P.-O. Studies in Perturbation Theory. IV. Solution of Eigenvalue Problem by Projection Operator Formalism. *J. Math. Phys.* **1962**, *3*, 969–982.

(65) Löwdin, P.-O. Studies in Perturbation Theory. *J. Mol. Spectrosc.* **1963**, *10*, 12–33.
(66) Löwdin, P.-O. Studies in Perturbation Theory: Part VI. Contraction of Secular Equations. *J. Mol. Spectrosc.* **1964**, *14*, 112–118.
(67) Priyadarshy, S.; Skourtis, S. S.; Risser, S. M.; Beratan, D. N. Bridge-Mediated Electronic Interactions: Differences between Hamiltonian and Green Function Partitioning in a Non-Orthogonal Basis. *J. Chem. Phys.* **1996**, *104*, 9473–9481.
(68) Kurnikov, I. V.; Beratan, D. N. Ab Initio Based Effective Hamiltonians for Long-Range Electron Transfer: Hartree–Fock Analysis. *J. Chem. Phys.* **1996**, *105*, 9561–9573.
(69) Schmidt, M. W.; Baldridge, K. K.; Boatz, J. A.; Elbert, S. T.; Gordon, M. S.; Jensen, J. H.; Koseki, S.; Matsunaga, N.; Nguyen, K. A.; Su, S.; Windus, T. L.; Dupuis, M.; Montgomery, J. A. General Atomic and Molecular Electronic Structure System. *J. Comput. Chem.* **1993**, *14*, 1347–1363.
(70) Pipek, J.; Mezey, P. G. A Fast Intrinsic Localization Procedure Applicable for Ab Initio and Semiempirical Linear Combination of Atomic Orbital Wave Functions. *J. Chem. Phys.* **1989**, *90*, 4916–4926.
(71) Berstis, L.; Baldridge, K. K. DFT-Based Green's Function Pathways Model for Prediction of Bridge-Mediated Electronic Coupling. *Phys Chem Chem Phys* **2015**, *17*, 30842–30853.
(72) Kobayashi, C.; Baldridge, K.; Onuchic, J. N. Multiple versus Single Pathways in Electron Transfer in Proteins: Influence of Protein Dynamics and Hydrogen Bonds. *J. Chem. Phys.* **2003**, *119*, 3550–3558.
(73) Onuchic, J. N.; Beratan, D. N. A Predictive Theoretical Model for Electron Tunneling Pathways in Proteins. *J. Chem. Phys.* **1990**, *92*, 722–733.
(74) Beratan, D. N.; Onuchic, J. N.; Winkler; Gray, H. B. Electron-Tunneling Pathways in Proteins. *Science* **1992**, *258*, 1740–1741.
(75) Seifert, G.; Porezag, D.; Frauenheim, T. Calculations of Molecules, Clusters, and Solids with a Simplified LCAO-DFT-LDA Scheme. *Int. J. Quantum Chem.* **1996**, *58*, 185–192.
(76) Porezag, D.; Frauenheim, T.; Köhler, T.; Seifert, G.; Kaschner, R. Construction of Tight-Binding-like Potentials on the Basis of Density-Functional Theory: Application to Carbon. *Phys. Rev. B* **1995**, *51*, 12947–12957.
(77) Elstner, M.; Porezag, D.; Jungnickel, G.; Elsner, J.; Haugk, M.; Frauenheim, T.; Suhai, S.; Seifert, G. Self-Consistent-Charge Density-Functional Tight-Binding Method for Simulations of Complex Materials Properties. *Phys. Rev. B* **1998**, *58*, 7260–7268.
(78) Gaus, M.; Cui, Q.; Elstner, M. DFTB3: Extension of the Self-Consistent-Charge Density-Functional Tight-Binding Method (SCC-DFTB). *J. Chem. Theory Comput.* **2011**, *7*, 931–948.
(79) Valeev, E. F.; Coropceanu, V.; da Silva Filho, D. A.; Salman, S.; Brédas, J.-L. Effect of Electronic Polarization on Charge-Transport Parameters in Molecular Organic Semiconductors. *J. Am. Chem. Soc.* **2006**, *128*, 9882–9886.
(80) Wesolowski, T.; Muller, R. P.; Warshel, A. Ab Initio Frozen Density Functional Calculations of Proton Transfer Reactions in Solution. *J. Phys. Chem.* **1996**, *100*, 15444–15449.
(81) Voorhis, T. V.; Kowalczyk, T.; Kaduk, B.; Wang, L.-P.; Cheng, C.-L.; Wu, Q. The Diabatic Picture of Electron Transfer, Reaction Barriers, and Molecular Dynamics. *Annu. Rev. Phys. Chem.* **2010**, *61*, 149–170.
(82) Dederichs, P. H.; Blügel, S.; Zeller, R.; Akai, H. Ground States of Constrained Systems: Application to Cerium Impurities. *Phys. Rev. Lett.* **1984**, *53*, 2512–2515.
(83) Wu, Q.; Van Voorhis, T. Direct Optimization Method to Study Constrained Systems within Density-Functional Theory. *Phys. Rev. A* **2005**, *72*, 24502–24506.
(84) Mulliken, R. S. Electronic Population Analysis on LCAO–MO Molecular Wave Functions. I. *J. Chem. Phys.* **1955**, *23*, 1833–1840.
(85) Löwdin, P.-O. On the Nonorthogonality Problem*. In *Advances in Quantum Chemistry*; Löwdin, P.-O., Ed.; Academic Press, 1970; Vol. 5, pp 185–199.

(86) Hirshfeld, F. L. Bonded-Atom Fragments for Describing Molecular Charge Densities. *Theor. Chim. Acta* **1977**, *44*, 129–138.
(87) CPMD Version 3.7.1, The CPMD Consortium, Http://Www.cpmd.org, MPI F"ur Festk"orperforschung and the IBM Zurich Research Laboratory.
(88) Köster, A. M.; Calaminici, P.; Casida, M. E.; Flores-Moreno, R.; Greudtner, G.; Goursot, A.; Heine, T.; Ipatov, A.; Janetzko, F.; del Campo, J. M.; Patchkovskii, S.; Reveles, J. U.; Vela, A.; Zuniga, B.; Salahub, D. *demon2K*; deMon developers: Cinvestav, Mexico City, 2006.
(89) Grimme, S. Semiempirical GGA-Type Density Functional Constructed with a Long-Range Dispersion Correction. *J. Comput. Chem.* **2006**, *27*, 1787–1799.
(90) Schäfer, A.; Huber, C.; Ahlrichs, R. Fully Optimized Contracted Gaussian Basis Sets of Triple Zeta Valence Quality for Atoms Li to Kr. *J. Chem. Phys.* **1994**, *100*, 5829–5835.
(91) Krishnan, R.; Binkley, J. S.; Seeger, R.; Pople, J. A. Self-consistent Molecular Orbital Methods. XX. A Basis Set for Correlated Wave Functions. *J. Chem. Phys.* **1980**, *72*, 650–654.
(92) Aradi, B.; Hourahine, B.; Frauenheim, T. DFTB+, a Sparse Matrix-Based Implementation of the DFTB Method †$. *J. Phys. Chem. A* **2007**, *111*, 5678–5684.
(93) Mintmire, J. W.; Dunlap, B. I. Fitting the Coulomb Potential Variationally in Linear-Combination-of-Atomic-Orbitals Density-Functional Calculations. *Phys. Rev. A* **1982**, *25*, 88–95.
(94) Calaminici, P.; Domínguez-Soria, V.-D.; Flores-Moreno, R.; Gamboa-Martínez, G. U.; Geudtner, G.; Goursot, A.; Salahub, D. R.; Köster, A. M. Auxiliary Density Functional Theory: From Molecules to Nanostructures. In *Handbook of Computational Chemistry*; Leszczynski, J., Ed.; Springer Netherlands, 2012; pp 573–610.
(95) Köster, A. M.; Reveles, J. U.; Campo, J. M. del. Calculation of Exchange-Correlation Potentials with Auxiliary Function Densities. *J. Chem. Phys.* **2004**, *121*, 3417–3424.
(96) Mejía-Rodríguez, D.; Köster, A. M. Robust and Efficient Variational Fitting of Fock Exchange. *J. Chem. Phys.* **2014**, *141*, 124114.
(97) Perdew, J. P.; Burke, K.; Ernzerhof, M. Generalized Gradient Approximation Made Simple. *Phys. Rev. Lett.* **1996**, *77*, 3865–3868.
(98) Tao, J.; Perdew, J. P.; Staroverov, V. N.; Scuseria, G. E. Climbing the Density Functional Ladder: Nonempirical Meta-Generalized Gradient Approximation Designed for Molecules and Solids. *Phys. Rev. Lett.* **2003**, *91*, 1464–-146404.
(99) Perdew, J. P.; Tao, J.; Staroverov, V. N.; Scuseria, G. E. Meta-Generalized Gradient Approximation: Explanation of a Realistic Nonempirical Density Functional. *J. Chem. Phys.* **2004**, *120*, 6898–6911.
(100) Adamo, C.; Barone, V. Toward Reliable Density Functional Methods without Adjustable Parameters: The PBE0 Model. *J. Chem. Phys.* **1999**, *110*, 6158–6170.
(101) Becke, A. D. Density-functional Thermochemistry. III. The Role of Exact Exchange. *J. Chem. Phys.* **1993**, *98*, 5648–5652.
(102) Zhao, Y.; Truhlar, D. G. The M06 Suite of Density Functionals for Main Group Thermochemistry, Thermochemical Kinetics, Noncovalent Interactions, Excited States, and Transition Elements: Two New Functionals and Systematic Testing of Four M06-Class Functionals and 12 Other Functionals. *Theor. Chem. Acc.* **2008**, *120*, 215–241.
(103) Zhao, Y.; Truhlar, D. G. Density Functional for Spectroscopy: No Long-Range Self-Interaction Error, Good Performance for Rydberg and Charge-Transfer States, and Better Performance on Average than B3LYP for Ground States. *J. Phys. Chem. A* **2006**, *110*, 13126–13130.
(104) Dunning Jr., T. H. Gaussian Basis Sets for Use in Correlated Molecular Calculations. I. The Atoms Boron through Neon and Hydrogen. *J. Chem. Phys.* **1989**, *90*, 1007–1023.
(105) Kendall, R. A.; Dunning Jr., T. H.; Harrison, R. J. Electron Affinities of the First-row Atoms Revisited. Systematic Basis Sets and Wave Functions. *J. Chem. Phys.* **1992**, *96*, 6796–6806.
(106) Woon, D. E.; Dunning Jr., T. H. Gaussian Basis Sets for Use in Correlated Molecular Calculations. III. The Atoms Aluminum through Argon. *J. Chem. Phys.* **1993**, *98*, 1358–1371.

(107) Calaminici, P.; Flores–Moreno, R.; Köster, A. M. A Density Functional Study of Structures and Vibrations of Ta_3O and Ta_3O^-. *Comput. Lett.* **2005**, *1*, 164–171.
(108) Köster, A. M.; Flores-Moreno, R.; Reveles, J. U. Efficient and Reliable Numerical Integration of Exchange-Correlation Energies and Potentials. *J. Chem. Phys.* **2004**, *121*, 681–690.
(109) Wu, Q.; Van Voorhis, T. Direct Calculation of Electron Transfer Parameters through Constrained Density Functional Theory. *J. Phys. Chem. A* **2006**, *110*, 9212–9218.
(110) Troullier, N.; Martins, J. L. Efficient Pseudopotentials for Plane-Wave Calculations. *Phys. Rev. B* **1991**, *43*, 1993–2006.
(111) Pilmé, J.; Luppi, E.; Bergès, J.; Houée-Lévin, C.; Lande, A. de la. Topological Analyses of Time-Dependent Electronic Structures: Application to Electron-Transfers in Methionine Enkephalin. *J. Mol. Model.* **2014**, *20*, 1–13.
(112) Pradie, N. A.; Linnert, H. V. Vertical and Adiabatic Ionization Potentials of Fluorinated, Chlorinated, and Chlorofluorinated Ethylenes Using G2 and G3 Theories. *J. Phys. Chem. A* **2007**, *111*, 4836–4848.